Assessment of Economic Recovery in Shanghai, China after the Pandemic Using Quarterly Nighttime Light Data

Feng Li 1,2, Xingjian Fu 1,2, Jiajun Li 1,2, Jinyu Zhang 1,2

College of Environment and Disaster Management, Institute of Disaster Prevention, 465 Xueyuan Street, Sanhe, China - lif1223@aliyun.com; 24661104@st.cidp.edu.cn; 1813778890@qq.com; 1753485303@qq.com
Hebei Key Laboratory of Earthquake Disaster Prevention and Risk Assessment, 465 Xueyuan Street, Sanhe, China

Keywords: COVID-19 pandemic, quarterly NPP-VIIRS data, nighttime light, economic recovery framework.

Abstract

The COVID-19 pandemic, which spanned from 2020 to 2022, significantly influenced socio-economic activities in Shanghai, China. Analysing the recovery of the Shanghai economy from the effects of the pandemic is crucial for understanding broader trends in China's economic development. A novel light correction index was developed by integrating nighttime light (NTL) data, point of interest (POI), the enhanced vegetation index (EVI), and population data. This index was subsequently combined with provincial quarterly GDP data to estimate county-level GDP. Economic recovery frameworks were then established for all districts in Shanghai to comprehensively assess their performance in recovering from the pandemic. The findings indicate that the novel light index effectively quantifies the intensity of human socio-economic activities while mitigating the oversaturation and blooming effects associated with NTL data. The average coefficient of determination (R^2) between the estimated county-level GDP and actual GDP is 0.801. Furthermore, the average R^2 for the developed economic recovery frameworks for the county-level districts before and after the pandemic is 0.948 and 0.748, respectively. These findings can serve as valuable indicators for assessing the economic recovery of Shanghai. It can be concluded that most districts in Shanghai demonstrated low economic resilience before and after the pandemic. Although the overall economy of Shanghai experienced growth, the growth rate was notably lower than the pre-pandemic level. As of the end of 2023, Shanghai's economy had not yet fully recovered to its pre-pandemic level.

1. Introduction

The outbreak of the novel coronavirus disease 2019 (COVID-19) in late 2019 exerted a profound impact on the Chinese economy, leading to a decrease in the growth rate from 5.9% in 2019 to 2.2% in 2020. To assess the impact of COVID-19 on the urban economy, it is crucial to investigate new perspectives that may aid policymakers in developing innovative and effective strategies for economic recovery. The existence of missing data and inconsistent statistical methods in traditional official statistics makes these large-scale datasets an inadequate representation of the real state of socio-economic activity within the administrative units of the sub-provinces. This hampers the efficient collection and management of economic data, ultimately adversely affecting the planning and operation of cities. The development of remote sensing technology and the rise of the big data era have laid the groundwork for humanity to explore the potential evolution of urban areas. The utilisation of remote sensing data, especially nighttime light (NTL) remote sensing data, presents a wide array of new possibilities for urban economic development (Gibson, et al., 2017), population (POP) distribution (Wu et al., 2021), energy consumption (Lei et al., 2024), carbon emissions (Wang et al., 2024), disaster assessment (Li et al., 2022), and other important fields. This is attributed to the data's inherent advantages of objectivity, timeliness, cost-effectiveness, and accessibility.

NTL data were employed extensively to assess the status of socio-economic and human activities during the pandemic. Elvidge et al. (2020) proposed that the pandemic led to a decrease in nighttime illumination and suggested that NTL can be used as a proxy variable to track changes in economic activity levels during downturns and recoveries. Xu et al. (2021) found an overall reduction in nighttime illumination after urban lockdown measures were implemented. Moreover, they

observed distinct regional variations and diverse spatial distributions of NTL. Specifically, the decline in NTL illumination was more notable in the urban areas than in the suburbs. Dasgupta (2022) used panel regression and machine learning to predict the year-on-year change in India's GDP in the first quarter of 2020. The method suggested that NTL and electricity consumption could be used as indicators of the state of the economy during the pandemic in the short term. Wang et al. (2022) revealed that COVID-19 had a far greater impact on developed Chinese cities than on less developed ones. As the pandemic was contained in March 2020, the extent of economic recovery varied throughout Chinese cities. Shao et al. (2021) investigated the fluctuations in nighttime illumination in Wuhan, China, before and after the 2020 pandemic. After the city lockdown was lifted, socio-economic activities in Wuhan experienced significant recovery, although production levels remained below the pre-pandemic norm. Tian et al. (2021) developed a work resumption index based on NTL data. As of March 2020, most cities in China reported work resumption indices exceeding 70%, with coastal cities demonstrating a more rapid resumption to activity in comparison to their interior counterparts. Li et al. (2024) utilised NTL data to evaluate the economic resilience of a city during the pandemic. The research revealed that economic resilience was highest in areas closer to the city's core.

The aforementioned studies focused on the initial stages of the pandemic and did not utilise NTL data to analyse urban economic recovery in the medium and long term. Li et al. (2023) evaluated the economic recovery of Hebei Province, China, at the provincial, prefectural, and county levels in 2021 using a counterfactual metric. Li et al. (2024) created a novel NTL index to explore the resilience and economic recovery of county-level districts in Beijing, China, before and after the pandemic. The pandemic lasted three years in China, resulting

in declining consumption, production, and investment and increasing local government debt. The urban economy of China has been significantly impacted by the global slowdown, resulting in adverse effects on investment, employment, and overall economic activity. Despite the significance of the topic, there seems to be a lack of comprehensive studies examining the post-pandemic trends and recovery of China's urban economy. Given that Shanghai is a key player in China's economic development, its post-pandemic economic recovery serves as an essential indicator for comprehending the broader economic landscape of the nation. To investigate the recovery state and economic resilience of the post-pandemic economy in Shanghai, China, this study established a county-level economic evaluation framework using long-term NTL time series and auxiliary data. The study's findings would assist decisionmakers in developing targeted economic recovery strategies.

2. Study Area and Data Sources

2.1 Study Area

Shanghai is situated in Eastern China, across from the Pacific Ocean and near the mouth of the Yangtze River (30°40′–31°53′ N, 120°51′– 122°12′ E), as depicted in Figure 1 (a) and Figure 1 (b). Shanghai has a subtropical monsoon climate with four distinct seasons, with an average altitude of 2.19 m and a maximum altitude of 103.7 m. It is China's financial and economic hub and is under the jurisdiction of 16 districts, with a population of 24,874,000 in 2023 and an area of 6340.5 km². The urban area of Shanghai encompasses the area enclosed by the Outer Ring Highway, highlighted by the green dashed line in Figure 1 (a). This area includes Huangpu, Xuhui, Changning, Jing'an, Putuo, Hongkou, and Yangpu districts, alongside portions of Pudong, Minhang, Baoshan, and Jiading districts.

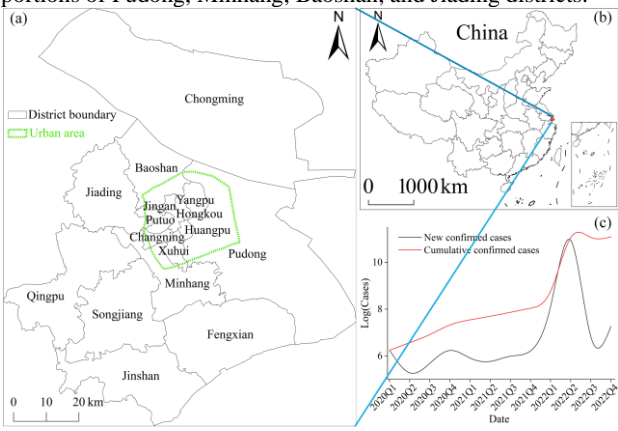


Figure 1. The geographical position of (a) Shanghai within (b) China, along with a graph illustrating (c) the quarterly new COVID-19 cases and the cumulative confirmed cases in the city throughout the pandemic.

From January 2020 to December 2022, a cumulative total of 65,598 cases of COVID-19 patients were diagnosed, and a cumulative total of 595 deaths were reported in Shanghai. The logarithm transformation of both new confirmed cases and the cumulative confirmed cases, depicted in Figure 1 (c), effectively illustrates the development trends of the pandemic. Shanghai experienced two major lockdown periods from 24 January to 23 March 2020 and from 28 March to 1 June 2022, respectively (Li et al., 2024). The pandemic shock of 2022 led to a 5.7% year-on-year decrease in Shanghai's GDP during the first half of the year. This megacity experienced a significant transformation in

its economic landscape and social development because of the profound effects of the pandemic.

2.2 Data Sources

This study relies on six primary categories of data sources: NPP-VIIRS data, MODIS13A1 products, point of interest (POI) data, POP data, GDP statistics, and administrative divisions.

3. Methodology

3.1 NTL Data Preprocessing

Firstly, monthly NPP-VIIRS composite data for every three months were averaged as quarterly NTL data. The quarterly NTL data may mistakenly categorize transient light sources and background noise as steady light sources, leading to decreased accuracy in the results. To eliminate stray light in the quarterly NTL data, a lower threshold for denoising the NTL image was determined by selecting and averaging the NTL image pixels within multiple large national watersheds. The NPP-VIIRS data is vulnerable to contamination from fires, gas flares, auroras, ships, biomass burning, and other temporary light sources. The maximum brightness observed in the central areas of megacities such as Beijing, Shanghai, and Guangzhou was selected as an upper threshold to filter out the extremely high values of these temporary lights (Mehak et al., 2024). The detailed equation used to filter NTL data noise is as follows:

$$NTL_{c} = \begin{cases} 0 &, NTL \leq NTL_{min} \\ NTL - NTL_{min} &, NTL_{min} \leq NTL \leq NTL_{max} \\ NTL_{max} - NTL_{min}, NTL > NTL_{max} \end{cases} \tag{1}$$

where NTL, NTL_c , NTL_{min} , and NTL_{max} denote the raw NTL, the denoised NTL, the lower threshold of NTL, and the upper threshold of NTL, respectively.

This study utilised panel data from 16 districts in Shanghai, covering the period from 2014 to 2023, to quantify the weights of the EANTLI, POI, and POP indicators using the Entropy Weight Method (EWM) (Wang et al., 2022). The results indicated that the average weights of the three indicators during the study period were 0.31, 0.36, and 0.33, respectively, with annual weights fluctuating slightly around 0.3 and a maximum difference of only 0.05. This suggests that the contributions of the three indicators to the research objectives were essentially equal, as the weight system exhibited no significant differentiation, confirming their equivalent importance within the evaluation framework. To effectively mitigate the oversaturation and blooming effects of NTLs in urban environments and to more comprehensively reflect the urban economic conditions closely related to human activity this study adopted an equal-weighting approach. It integrates EANTLI, POI, and POP data to develop the EVI, POI, and POP-Adjusted NTL Index (EPPANI). The specific calculation equation for EPPANI is as follows:

$$EPPANI = \sqrt{\frac{1 + NTL_n - EVI_a}{1 - NTL_n + EVI_a} \times NTL_n \times POI \times POP}$$
 (2)

where EVI_a indicates the annual average EVI.

3.2 Estimation of County-Level Quarterly GDP

Related research indicates a strong correlation between NTL data and regional socio-economic development (Wu et al., 2024; Li et al., 2024). However, a more precise understanding of the relationship between the two is still lacking. Thus, there is a need for an objective, rational, and practical method to perceive the level of socio-economic development based on NTL data. Firstly, the sum of EPPANI across all 31 provincial administrative divisions in China was denoted as SE. Next, the quadratic polynomial relationship between SE and QGDP with an intercept of 0 was established according to the principle of "no light, no GDP". The quadratic polynomial equation is expressed as follows:

$$QGDP_i = a \cdot SE_i^2 + b \cdot SE_i \tag{3}$$

where $QGDP_i$ and SE_i denote the real quarterly GDP and EPPANI sum of the i^{th} province, respectively; a and b denote the coefficients of the quadratic polynomial, respectively.

Employing the top-down quadratic polynomial model mentioned above to estimate QGDP at the pixel level inevitably yields large estimation errors. To address this problem, the estimated GDP for each pixel within a provincial administrative unit was corrected using the following GDP correction equation:

$$P_j^{\rm c} = P_j \times \frac{P_{\rm R}}{P_{\rm F}} \tag{4}$$

where P_j^c and P_j denote the corrected QGDP of pixel j and the QGDP of pixel j estimated using the quadratic polynomial model, respectively; PR and PE denote the real QGDP of the specific province and the QGDP of the same province estimated using the quadratic polynomial model, respectively.

The corrected pixel-level QGDP for the county-level administrative districts of Shanghai was aggregated to determine the QGDP for each district.

3.3 Economic Recovery Framework after the Pandemic

China's quarterly GDP data reveal a distinct cyclical pattern, highlighting the influence of seasonal factors on GDP across various years within a specific timeframe. This seasonal volatility significantly disrupts the performance of the Chinese economy, making it essential to exclude these fluctuations when analysing changes in GDP. Therefore, seasonal and trend decomposition using Loess (STL) was adopted to improve the forecasting accuracy of time-series GDP. As a classical time-series decomposition method, STL decomposes time-series data into three key components: trend, seasonal, and residuals. Moreover, it offers a more robust analysis for time series with outliers (Tam et al., 2024). The most used STL method is the additive model, which uses the following equation:

$$P_{t} = T_{t} + S_{t} + R_{t} \quad t = 1, \dots, N$$
 (5)

where P_t denotes an observation series with N GDP data at period t; Tt denotes the trend component which reflects the long-term fluctuations within the series; S_t denotes the seasonal component reflecting seasonal variation; R_t denotes the irregular component (noise), describing random, irregular influences.

To assess the recoverability of the study area, we analysed the trend component and developed a framework for potential economic recovery following the pandemic, as illustrated in Figure 2. The post-pandemic economic recovery framework outlined four potential patterns of economic recovery after the pandemic: strong growth, sustainable growth, contractionary growth, and downturn. The strong growth pattern indicates that the economy of the study area was only marginally impacted by the pandemic. Owing to its remarkable economic resilience, the study area not only surpassed its pre-pandemic growth rates but also demonstrated a rapid economic recovery, indicating a strong trajectory of economic development. The sustainable growth pattern describes the initial phase of the pandemic where GDP grew rapidly, followed by a dramatic slowdown due to the shock of the pandemic, and then a vigorous rebound once pandemic restrictions were eased, ultimately revealing a robust upward trend overall. The contractionary growth pattern indicates that the economy of the study area suffered immensely due to the pandemic, resulting in a substantial decrease in economic growth compared to the pre-pandemic levels. Moreover, predicting the timeline for economic recovery under such an economic context remains challenging. The downturn pattern indicates that the economy initially experienced a decline due to the pandemic shock, followed by a phase of rapid growth. However, the absence of sustained momentum in this growth ultimately resulted in a downward trend even after the lockdown measures were lifted.

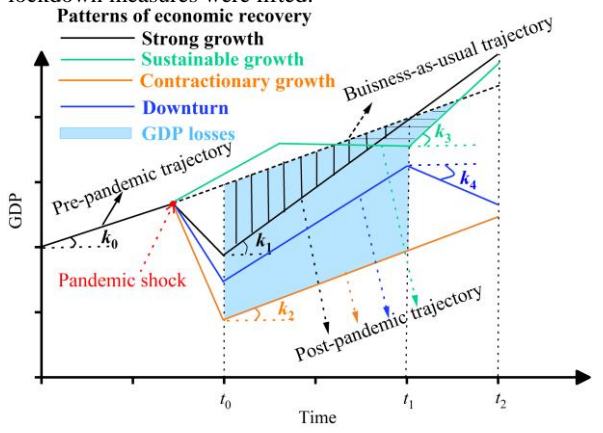


Figure 2. Potential frameworks for economic recovery after the pandemic.

As illustrated in Figure 2, the black solid line before time t0 represents the GDP trajectory before the pandemic, whereas the black short dashed line following time t_0 represents the GDP trajectory that would occur in the absence of the pandemic, known as the business-as-usual trajectory [30]. The black solid line before time t0 represents the pre-pandemic GDP trajectory, spanning from the first quarter of 2014 to the fourth quarter of 2019. In contrast, the black short dashed line following time t0 represents the GDP trajectory that would have occurred in the absence of the pandemic. Meanwhile, the green, black, blue, and brown solid lines following time t_0 represent the postpandemic GDP trajectories, spanning from the first quarter of 2020 to the fourth quarter of 2023. When the slope of the postpandemic GDP trajectory (k_1 and k_3) is greater than the slope of the pre-pandemic GDP trajectory (k_0) , it indicates a promising economic rebound for the region. On the other hand, if the slope of the post-pandemic GDP trajectory (k_2 and k_4) is less than or equal to k_0 , it indicates that the region's economy is experiencing slower growth or decline, suggesting that an economic recovery within a specific timeframe is impossible. To effectively capture the economic development trends of the region before and after the pandemic, a comprehensive analysis

and comparison of various regression models—including linear, quadratic polynomial, cubic polynomial, power function, and exponential function models—was conducted. By applying comprehensive statistical analyses, including the F-test, t-test, p-value, and coefficient of determination (R^2), the optimal regression model was determined to accurately represent the trajectory of economic development before and after the pandemic.

Given that the strong and sustainable growth pattern demonstrates a higher economic growth rate in the post-pandemic period compared to the pre-pandemic period, the regional economy is expected to recover in the short or medium term. Moreover, the regional economic losses can be estimated by comparing the business-as-usual trajectory and the post-pandemic GDP trajectory. Cumulative economic losses are used to measure the regional economic losses caused by the pandemic and are qualified using the following equation:

$$C = \int_{t_{0}}^{t_{r}} [T_{a}(t) - T_{b}(t)]dt$$
 (6)

where C denotes the cumulative economic losses; tr denotes the end of the GDP recovery phase (t_1) or the end of the study phase (t_2) ; $T_a(t)$ and $T_b(t)$ denote the business-as-usual and post-pandemic GDP development trajectories, respectively.

4. Results

4.1 Validation of Estimated County-Level GDP

A quadratic polynomial regression model was employed to examine the relationship between provincial EPPANI and quarterly GDP, spanning from the first quarter of 2014 to the fourth quarter of 2023. The R^2 varies between 0.717 and 0.925, with an average of 0.835. Additionally, the estimated annual GDP was calculated by aggregating the four quarterly GDP figures. This estimated annual GDP was then integrated with the actual annual GDP data to construct a linear regression model, which assesses the quarterly GDP estimates at the county level in Shanghai. The model was used to analyse the consistency between estimated GDP and actual GDP data across 16 districts in Shanghai from 2014 to 2023. The R^2 values of the model for these 16 districts range from 0.436 to 0.890, with an average value of 0.801, as illustrated in Table 1. As shown in Table 1, the values for predicted R2, MAE (Mean Absolute Error), and RMSE (Root Mean Square Error) in 2021 are remarkably high. The COVID-19 pandemic lockdown had a profound impact on the Lujiazui financial district, commercial centres, tourist attractions, and Pudong International Airport along the east bank of the Huangpu River, resulting in a marked decline in human activities throughout Pudong New Area in 2021. Consequently, the estimated GDP for Pudong New Area diverged significantly from the official GDP figures, contributing to a reduced R^2 value in the linear regression analysis. Overall, there is a strong correlation between the estimated quarterly county-level GDP and the actual GDP, indicating that EPPANI serves as a dependable tool for estimating quarterly county-level GDP.

Year	R^2	MAE	RMSE
2014	0.872	445.808	630.248
2015	0.871	488.702	702.753
2016	0.880	520.967	815.226
2017	0.848	611.846	977.402

2018	0.890	647.759	880.805
2019	0.870	759.929	1252.228
2020	0.654	1069.068	1914.445
2021	0.436	1389.096	2657.599
2022	0.864	914.775	1738.355
2023	0.811	1097.108	1998.811

Table 1. The R^2 , MAE, and RMSE of the linear regression between the estimated annual GDP and the actual annual GDP from 2014 to 2023.

4.2 Validation of Economic Recovery Models

The relative errors associated with the seasonal component Tt and the estimated quarterly GDP of the economic recovery model for Shanghai, both before and after the pandemic, are 2.5% and 2.1%, respectively. The model demonstrates an impressive R^2 of 0.972 before the pandemic and 0.950 postpandemic, along with F-values of 757.17 and 266.42. Notably, the p-values consistently remain at 0.0, highlighting the robustness of the results. The relative errors associated with the seasonal decomposition of the estimated GDP for the districts of Shanghai are illustrated in Table 2. Before the pandemic, the relative errors between the trend component T_t and the estimated quarterly GDP exhibited a minimum of 1.3%, a maximum of 5.9%, and an average of 3.3%, respectively. In contrast, following the pandemic, these figures changed to 2.1% for the minimum, 6.6% for the maximum, and 3.8% for the average. The estimated GDP of the Pudong New Area in 2021 was relatively low, resulting in the largest relative error of 6.6% in the trend component T_t following the pandemic. Despite this larger error, it does not compromise the accuracy of the economic recovery model for the Pudong New Area.

	Dalativa Erman (0/)		
District	Relative Error (%)		
Bistrict	Pre-pandemic	Post-pandemic	
Huangpu	2.7	3.4	
Xuhui	1.3	2.1	
Changning	1.8	3	
Jing'an	1.6	2.1	
Putuo	1.3	2.1	
Hongkou	2.3	3.1	
Yangpu	3.1	3.3	
Minhang	4.5	3.7	
Baoshan	3	3.2	
Jiading	5.2	3.9	
Pudong	3.9	6.6	
Jinshan	5.9	5.9	
Songjiang	3.2	4	
Qingpu	3.1	3.9	
Fengxian	5.6	4.9	
Chongming	5.1	5.5	

Table 2. The relative errors associated with the seasonal decomposition of the estimated GDP for the districts of Shanghai.

The pre-pandemic regression models for GDP show R^2 ranging from 0.850 to 0.992 and F-values ranging from 155.348 to 2822.679, with p-values remaining at 0.00. The post-pandemic

regression models for GDP show R^2 ranging from 0.612 to 0.952 and F-values ranging from 6.313 to 276.618, with p-values remaining at 0.00. The results of these errors demonstrate that both pre- and post-pandemic GDP forecasting models are reliable, serving as effective tools to assess the recovery of the Shanghai county-level economy.

4.3 Assessment of Economic Recovery in Shanghai

The economic recovery framework of Shanghai under the impact of the pandemic is shown in Figure 3. Before the pandemic, Shanghai's GDP followed an exponential growth trajectory; however, post-pandemic, its GDP had shifted to a linear trajectory. Figure 3 shows that GDP growth in Shanghai has significantly declined since the pandemic, indicating that by the end of 2023, the economy in Shanghai has not recovered to pre-pandemic levels.

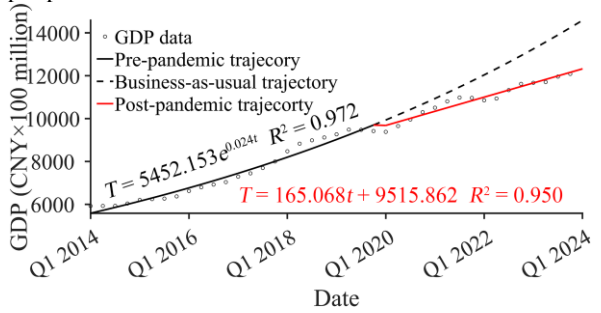
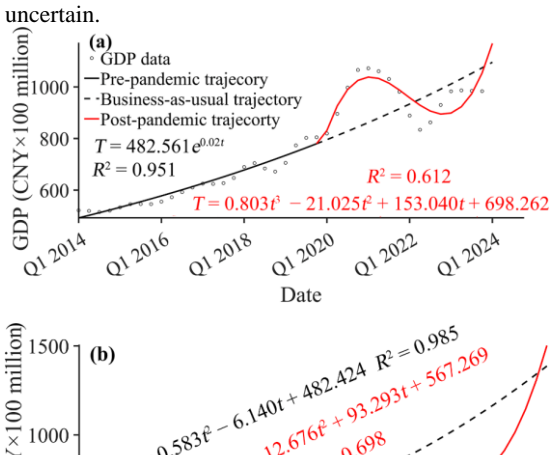


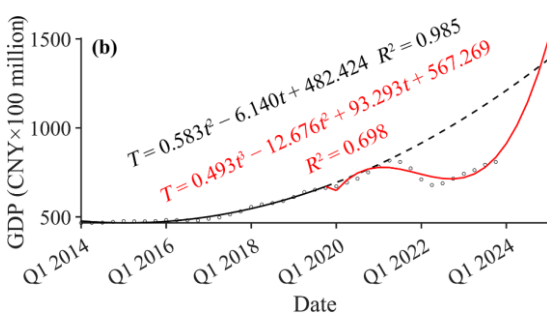
Figure 3. The economic recovery framework of Shanghai, China, under the impact of the pandemic.

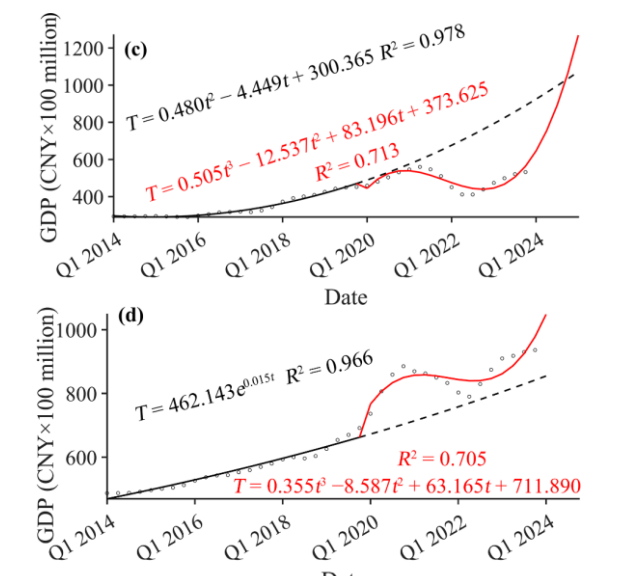
The economic recovery framework for the 16 districts of Shanghai under the impact of the pandemic is illustrated in Figure 4. Before the pandemic, Xuhui, Changning, Hongkou, and Qingpu districts demonstrated a quadratic polynomial growth pattern, while Putuo and Songjiang districts followed a linear growth pattern. In contrast, the other ten districts exhibited an exponential growth pattern. Following the pandemic, Shanghai's economic development model revealed a diverse array of patterns, encompassing cubic polynomials, quadratic polynomials, linear functions, power functions, and exponential functions. Jiading, Jinshan, Songjiang, and Chongming districts exhibited a power function growth pattern, while Minhang and Pudong New Area followed a linear growth pattern. On the other hand, Qingpu District showcased an exponential growth pattern, and Fengxian District revealed a quadratic polynomial decline pattern. Meanwhile, the economic development of the remaining eight districts displayed a cubic polynomial growth pattern.

As illustrated in Figure 4 (k), the pandemic profoundly affected the economy of Pudong New Area, leading to a staggering economic loss estimated at 4285.0994 billion CNY. However, following the pandemic, the district's economy has shown remarkable resilience and a strong growth pattern, with expectations for a complete recovery by the third quarter of 2032. As illustrated in Figure 4 (a), (b), (c), (d), (e), (f), (g), and (i), the economies of Huangpu, Xuhui, Changning, Jing'an, Putuo, Hongkou, Yangpu, and Baoshan exhibited a distinct trajectory of initial growth, subsequent decline, and then a swift rebound, largely influenced by the impacts of the pandemic. The economy of Jing'an District demonstrated remarkable resilience during the pandemic, as its post-pandemic economic recovery trajectory surpassed the expected business-as-usual trajectory. The anticipated economic losses for Huangpu, Xuhui,

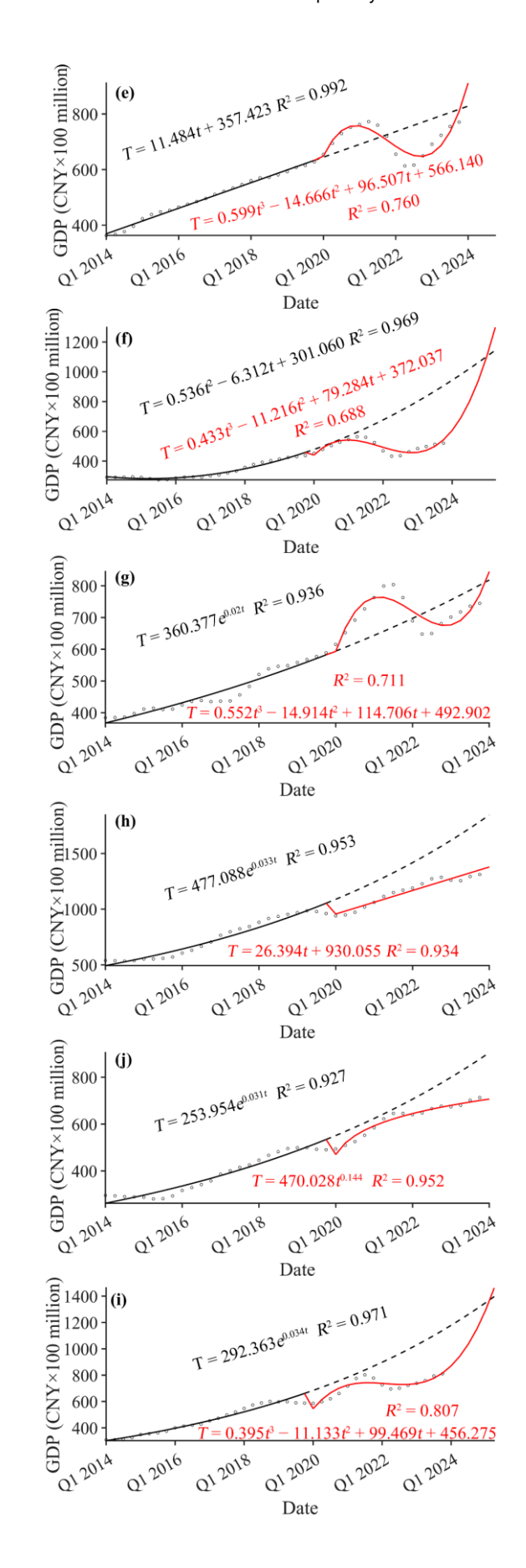
Changning, Putuo, Hongkou, Yangpu, and Baoshan are as follows: 50.2911 billion CNY, 335.1742 billion CNY, 345.4344 billion CNY, 69.8746 billion CNY, 377.65067 billion CNY, 36.87645 billion CNY, and 375.73542 billion CNY. The economies of these districts are expected to recover in the first quarter of 2024, the first quarter of 2024, the fourth quarter of 2024, the first quarter of 2024, the first quarter of 2025, the first quarter of 2024, and the first quarter of 2025, respectively. As illustrated in Figure 4 (h), (j), (l), (m), (n), and (p), the economies of Minhang, Jiading, Jinshan, Songjiang, Qingpu, and Chongming were experiencing growth in the aftermath of the pandemic. However, the slope of their economic recovery trajectories was notably lower than that of the pre-pandemic business-as-usual trajectories. Furthermore, the economic recovery models for these districts reveal contractionary growth patterns, leaving the timeline for a full recovery shrouded in uncertainty. As illustrated in Figure 4 (o), the pandemic significantly influenced the economy of Fengxian District, leading to an initial growth trend that was subsequently followed by a decline. The overall economic recovery had been downward, and the timeline for a full recovery remained







Date



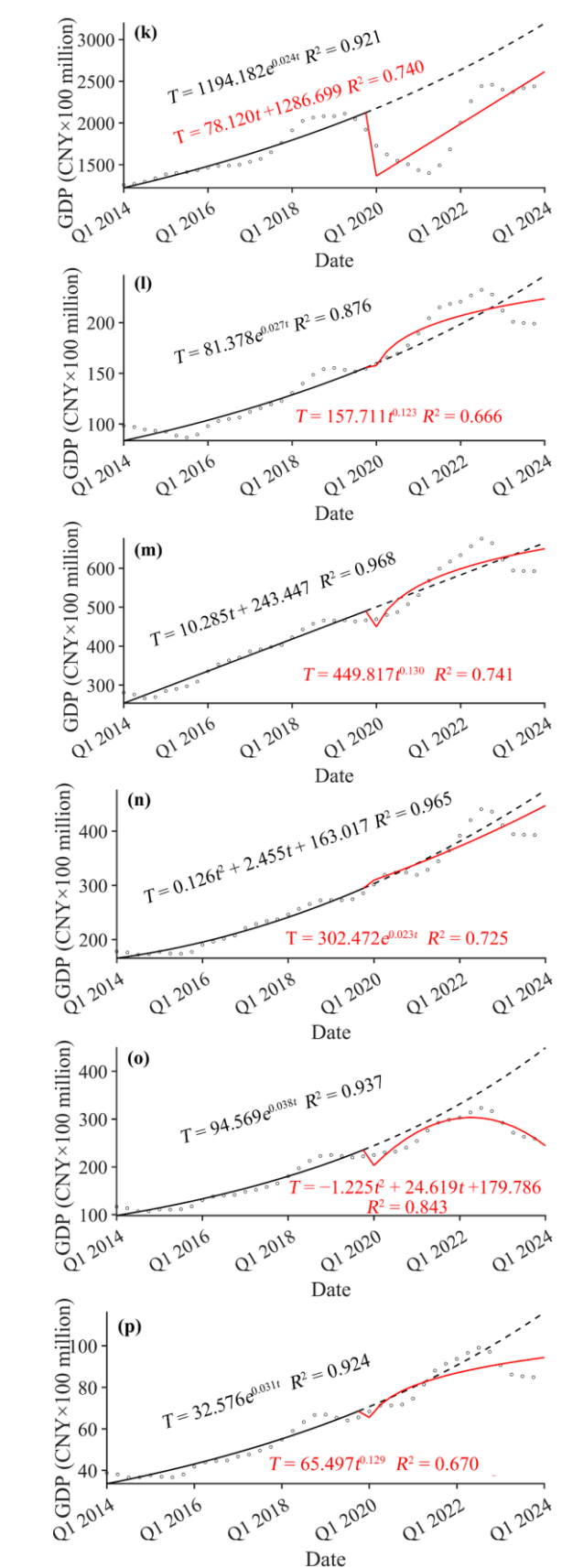


Figure 4. Frameworks for economic recovery under the impact of the pandemic in (a) Huangpu, (b) Xuhui, (c) Changning, (d) Jing'an, (e) Putuo, (f) Hongkou, (g) Yangpu, (h) Minhang, (i) Baoshan, (j) Jiading, (k) Pudong, (l) Jinshan, (m) Songjiang, (n) Qingpu, (o) Fengxian, and (p) Chongming.

4.4 Economic Impact of the Pandemic on Different Urban Areas

As illustrated in Figure 4 (a), (b), (c), (d), (e), (f), (g), and (i), the post-pandemic economic recovery trajectories of Huangpu, Xuhui, Changning, Jing'an, Putuo, Hongkou, Yangpu, and Baoshan were extremely similar. Following the pandemic, these districts faced a sharp economic downturn due to lockdown measures. However, after the lockdown measures were lifted in the second quarter of 2020, they witnessed a remarkable rebound. This economic upward trend was short-lived, as rising COVID-19 infections in the first quarter of 2021 led to renewed lockdown measures, causing a subsequent economic decline. The situation worsened in the second quarter of 2022, when the strictest home quarantine regulations were imposed, plunging the economies of these districts to their lowest levels. This indicates that the lockdown measures implemented during the pandemic played a key role in shaping economic development in the urban areas of Shanghai. As illustrated in Figure 4 (h), (j), (k), (l), (m), (n), (o), and (p), the post-pandemic economic recovery trajectories of Minhang, Jiading, Pudong, Jinshan, Songjiang, Qingpu, Fengxian, and Chongming were quite similar. Following the pandemic, the economies of these districts initially experienced a decline but later showed signs of recovery. Minor lockdown measures had little effect on the economic growth of these suburbs until the second quarter of 2022, when the implementation of full lockdown measures led to a steep decline in their economies. Despite the complete lifting of these restrictions at the end of 2022, these districts with ongoing severe economic challenges, characterized by sluggish economic development and an ambiguous path to full economic recovery. Minor pandemic lockdown measures exerted a diminished impact on the suburban economy. The suburbs often face limited opportunities for economic growth compared to their urban counterparts. Following the pandemic, the momentum for economic development in these suburbs tended to diminish, making it increasingly difficult to forecast the timing of their economic recovery.

5. Discussion

The transit time of NPP-VIIRS satellite is at 1:30 a.m. local time, which coincides with the power shutdown of numerous urban facilities and residential areas in the early morning hours. As a result, the NTL illumination captured by this satellite will likely appear dimmed. Moreover, the varying heights of buildings in urban environments can obstruct artificial light rays from multiple satellite perspectives. This phenomenon leads to a more pronounced angular effect in densely populated urban centres than in suburban or rural areas, ultimately reducing the overall illumination of NTL. During the pandemic, local government-mandated lockdown measures led to a surge in illumination in residential areas, while concurrently reducing illumination in industrial and commercial areas. Furthermore, the high albedo of winter snow in North China enhances the reflection of lunar radiation, greatly increasing the surface radiance of this region. As a result, this effect noticeably intensifies the regional NTL illumination. The aforementioned alterations in NTL illumination can result in exaggerated or diminished GDP estimates, compromising the reliability of models intended to assess the recovery of urban economies following the pandemic. The problem of NTL over- and underestimation of GDP can be effectively mitigated by incorporating POI and POP data. However, the local government's implementation of various economic support policies during or after the pandemic could introduce considerable uncertainty into the pandemic recovery framework, potentially impacting the effectiveness of the regional economic recovery assessments.

6. Conclusions

The NPP-VIIRS NTL monthly composite data is widely regarded as an exceptional resource for assessing socio-economic conditions. However, its effectiveness is hindered by its low spatial resolution, which restricts its full potential. This study introduces an innovative NTL correction index, EPPANI, which effectively integrates NTL, EVI, POP, and POI data with provincial quarterly GDP data to provide a more accurate estimation of quarterly GDP at the county level. Through visual comparison analysis, EPPANI demonstrates its capability to accurately reflect human socio-economic activities while greatly reducing the problems associated with the oversaturation and blooming effect of NTL data.

The average correlation coefficient between estimated GDP and actual GDP across 16 districts in Shanghai, as measured by the EPPANI index, is as high as 0.801. Additionally, the average R2 of regression models for GDP forecasts before and after the pandemic are 0.943 and 0.748, respectively. These findings underline the robustness of the economic recovery framework established for Shanghai in response to the pandemic's challenges.

The analysis of Shanghai's economic recovery framework following the pandemic reveals a complex landscape. Throughout the pandemic, lockdown measures exerted a greater impact on the urban areas of Shanghai compared to the suburban areas. However, after the pandemic, the suburban areas experienced a slower economic recovery than their urban counterparts. While only one district remained unscathed by the pandemic's impacts and eight districts exhibit predictable recovery timelines, seven districts continue to experience growth rates below the pre-pandemic norm. Considering the waning economic resilience of Shanghai during and after the pandemic, it is improbable that the city's economy will be restored to its pre-pandemic levels by the end of 2023. This is particularly evident when noting that, although the Shanghai economy is experiencing overall growth, it remains below the rates observed before the pandemic.

Funding

This work was funded by the Hebei Key Laboratory of Earthquake Disaster Prevention and Risk Assessment, grant number FZ247105; the National Key Research and Development Program of China, grant number 2017YFD0300403.

References

Dasgupta, N., 2022: Using Satellite Images of Nighttime Lights to Predict the Economic Impact of COVID-19 in India. Advances in Space Research, 70(4), 863-879. doi.org/10.1016/j.asr.2022.05.039.

Elvidge, C.D., Ghosh, T., Hsu, F.-C., Mikhail, Z., Bazilian, M., 2020: The Dimming of Lights in China during the COVID-19 Pandemic. *Remote Sensing*, 12(17), 2851. doi.org/10.3390/rs12172851.

Gibson, J., Olivia, S., Boe-Gibson, G., Li, C., 2021: Which Night Lights Data Should We Use in Economics, and Where?

- Journal of Development Economics, 149, 102602. doi.org/10.1016/j.jdeveco.2020.102602.
- Lei, Y., Xu, C., Wang, Y., Liu, X., 2024: Grid Model of Energy Consumption Using Random Forest by Integrating Data on the Nighttime Light, Population, and Urban Impervious Surface (2000–2020) in the Guangdong–Hong Kong–Macau Greater Bay Area. *Energies*, 17(11), 2518. doi.org/10.3390/en17112518.
- Li, Y., Hao, S., Han, Q., Guo, X., Zhong, Y., Zou, T., Fan, C., 2024: Study on Urban Economic Resilience of Beijing, Tianjin and Hebei Based on Night Light Remote Sensing Data during COVID-19. *Science of Remote Sensing*, 9, 100126. doi.org/10.1016/j.srs.2024.100126.
- Li, F., Liao, S., Liu, W., 2024: Assessment of Post-Pandemic Economic Recovery in Beijing, China, Using Night-Time Light Data. *Remote Sensing Letters*, 15(6), 603-613. doi.org/10.1080/2150704x.2024.2359098.
- Li, F., Liu, J., Zhang, M., Liao, S., Hu, W., 2023: Assessment of Economic Recovery in Hebei Province, China, under the COVID-19 Pandemic Using Nighttime Light Data. *Remote Sensing*, 15(1), 22. doi.org/10.3390/rs15010022.
- Li, F., Wang Q., Hu W., Liu J., Zhang X., 2022: Rapid Assessment of Disaster Damage and Economic Resilience in Relation to the Flooding in Zhengzhou, China in 2021. *Remote Sensing Letters*, 13(7), 651-662. doi.org/10.1080/2150704x.2022.2068987.
- Li, Y., Wang, S., 2024: Exploration of Eco-Environment and Urbanization Changes Based on Multi-Source Remote Sensing Data—A Case Study of Yangtze River Delta Urban Agglomeration. *Sustainability*, 16, 5903. doi.org/10.3390/su16145903.
- Li, Y., Yang, Y., Zhang, L., 2024: Comparison of Air Pollutants during the Two COVID-19 Lockdown Periods in Winter 2019 and Spring 2022 in Shanghai, China. *Atmosphere*, 15, 443. doi.org/10.3390/atmos15040443.
- Mehak, J., Gupta, P.K., Srivastav, S.K., 2024: Generation of Monthly VIIRS Nighttime Lights Time-Series (1992-2013) Images Using Deep Learning (cGAN) Technique. *Remote Sensing Applications: Society and Environment*, 35, 101263. doi.org/10.1016/j.rsase.2024.101263.
- Shao, Z., Tang, Y., Huang, X., Li, D., 2021: Monitoring Work Resumption of Wuhan in the COVID-19 Epidemic Using Daily Nighttime Light. *Photogrammetric Engineering & Remote Sensing*, 87(3), 195-294. doi.org/10.14358/pers.87.3.197.
- Tian, S., Feng, R., Zhao, J., Wang, L., 2021: An Analysis of the Work Resumption in China under the COVID-19 Epidemic Based on Night Time Lights Data. *ISPRS International Journal of Geo-Information*, 10(9), 614. doi.org/10.3390/ijgi10090614.
- Tam, B.C.M., Tang, S.-K., Cardoso, A., 2024: MTS Decomposition and Recombining Significantly Improves Training Efficiency in Deep Learning: A Case Study in Air Quality Prediction over Sub-Tropical Area. *Atmosphere*, 15, 521. doi.org/10.3390/atmos15050521.
- Wang, G., He, L., Guo, J., Huang, J., 2024: The Estimation of Building Carbon Emission Using Nighttime Light Images: A

- Comparative Study at Various Spatial Scales. *Sustainable Cities and Society*, 101, 105066. doi.org/10.2139/ssrn.4463901.
- Wang, Y., Teng, F., Wang, M., Li, S., Lin, Y., Cai, H., 2022: Monitoring Spatiotemporal Distribution of the GDP of Major Cities in China during the COVID-19 Pandemic. *International Journal of Environmental Research and Public Health*, 19(13), 8048. doi.org/10.3390/ijerph19138048.
- Wang, M., Wang, Y., Teng, F., Li, S., Lin, Y., Cai, H., 2022: China's Poverty Assessment and Analysis under the Framework of the UN SDGs Based on Multisource Remote Sensing Data. *Geo-Spatial Information Science*, 27 (1), 111–131. doi:10.1080/10095020.2022.2108346.
- Wu, N., Yan, J., Liang, D., Sun, Z., Ranjan, R., Li, J., 2024: High-Resolution Mapping of GDP Using Multi-Scale Feature Fusion by Integrating Remote Sensing and POI Data. *International Journal of Applied Earth Observation and Geoinformation*, 129, 103812. doi.org/10.1016/j.jag.2024.103812.
- Wu, B., Yang, C., Wu, Q., Wang, C., Wu, J., Yu, B., 2023: A Building Volume Adjusted Nighttime Light Index for Characterizing the Relationship between Urban Population and Nighttime Light Intensity. *Computers, Environment and Urban Systems*, 99, 101911. doi.org/10.1016/j.compenvurbsys.2022.101911.
- Xu, G., Xiu, T., Li, X., Liang, X., Jiao, L., 2021: Lockdown Induced Night-Time Light Dynamics during the COVID-19 Epidemic in Global Megacities. *International Journal of Applied Earth Observation and Geoinformation*, 102: 102421. doi.org/10.1016/j.jag.2021.102421.